Bi-doped $CH_3NH_3PbI_3$ effective masses and electronic properties research: A theoretical study using VASP

Liping Peng*

School of Mathematics and Physics, Huanggang Normal University, Newport NO.2 Road, Hubei, Huanggang, 438000, P.R. China

*Corresponding author: Fax: (+86) 0713-8835186; E-mail: pengliping@hgnu.edu.cn

DOI: 10.5185/amlett.2019.2232
www.vbripress.com/aml

Abstract

We calculated the effective masses and electronic properties of Bi-doped $CH_3NH_3PbI_3$ perovskites as a thermoelectric material using the VASP functional. The Bismuth doping concentration of 11.1%, 20%, and 33.3% corresponding band gaps are 1.46. 0.75, 0.56 eV, respectively. The effective masses of carriers and the band gaps decrease with the doping concentration addition. We found that the structure of Bi as an interstitial atom doped $MAPbI_3$ were much more stable than undoped one by the crystal systemic energy, and the Bi doping made the Fermi Level shift close to the bottom of conduction band, leading to charge carrier close to the Fermi level, resulted in the higher electrical conductivity. Moreover, Bi doping produced a smaller electron effective mass with doping concentration addition, increasing the $MAPbI_3$'s mobility. As a result, the Bi-doped $MAPbI_3$ could simultaneously enhance the electrical conductivity and Seebeck coefficient. Our results showed that Bi doped $MAPbI_3$ is a promising approach to develop thermoelectric and photovoltaic properties in organic-inorganic hybrid perovskite materials. Copyright © 2019 VBRI Press.

Keywords: Bi-doped $MAPbI_3$, effective masses, electrical conductivity, seebeck coefficient, fermi level.

Introduction

The solar cells based on hybrid organic-inorganic halide perovskite (e.g., $CH_3NH_3PbX_3$ or $MAPbX_3$, X = Cl, Br, I) as light absorbers are upcoming new players in the field of third-generation photovoltaics [**1-6**]. In the past 2 years, pervoskite-type methylammonium lead halides emerged as light harvesters for mesoscopic heterojunction solar cells, reaching a surprisingly high energy conversion efficiency of about 23.3%, comparable to that of the commercial silicon solar cells [**7−9**]. References [**10-12**] have developed different technologies to make sandwich-type absorbers, exhibiting the direct band gap, large absorption coefficient, and high carrier mobility. The previous investigations of the physical properties (e.g., electronic structure and optical properties) of hybrid organic-inorganic perovskites to some extent explained why they are so promising for solar energy conversion [**13-16**]. As we know, lead poisoning is a type of metal poisoning and a medical condition in humans and vertebrates caused by increased levels of the heavy metal lead in the body; moreover, lead interferes with a variety of body processes and is toxic to many organs and tissues, including the heart, bones, intestines, kidneys, and reproductive and nervous systems [**17**]. However, all of these advanced materials contain the toxic element lead, which would eventually hinder the commercialization of the products in the market. Bismuth (Bi) is in element the same group as lead, and it would be interesting to study the effects of replacing the Pb in methylammonium lead halides by Bi. In this report, we have investigated the effective masses of hole and electron at the Γ point and the electronic properties of nontoxic methylammonium Bi halide ($CH_3NH_3Pb_{1-x}Bi_xI_3$) compounds using the Vienna Ab-inito Simulation Package [**18**].

Details calculation methods

First-principles study of the Bi-doped $MAPbI_3$ was performed. The electrical structure properties was investigated base on the Density Functional Theory (DFT) and the VASP (Vienna Ab-inito Simulation Package) program. We used plane wave to unfold wave function, the cut off energy was 400 eV, the K point in brillouin zone was 6×6×6, and each atom stress was lower than 0.01 eV/Å. In the different phase structure materials, because between the organic ion and inorganic ion have not produce the new chemical bond, they are connect by the Van der Waals correction (vdW-DF) **[19]**, the exchange correlation energy used the Perdew-Burke-Ernzercof Generalized Gradient Approximation (GGA-PBE) [**20**]. In addition, we know that the spin-orbit coupling effect has an effect for the bandgap, especially, it has a strong effect to the heavy metal element's material system. Here, we can't neglect the spin-orbit

Copyright © 2019 VBRI Press

coupling effect in the $CH_3NH_3PbI_3$ system. Therefore, we calculated the energy band, density of state, and optical properties by the GGA-PBE and vdW-DF methods with the spin-orbit coupling effect in our calculation.

Similar to $CH_3NH_3PbX_3$ (X=halogens), $CH_3NH_3Pb_{1-x}Bi_xI_3$ also exhibits a very rich phase diagram as a function of temperature, i.e., the crystal structure goes from cubic, tetragonal, orthorhombic, and monoclinic to triclinic class by cooling [**21-26**]. The complicated phase transition behaviors of $CH_3NH_3Pb_{1-x}Bi_xI_3$ structure is attributed to the disordering of $(CH_3NH_3)^+$ cations and the distortions of $(Pb_{1-x}Bi_xI_3)^-$ octahedra at finite temperature [**21-24, 26**]. For example, in the high-temperature cubic phase, the orientations of $(CH_3NH_3)^+$ cations are completely disordered. In the same phase, the $Pb_{1-x}Bi_xI_6$ structural unit has perfect cubic symmetry. By lowering the temperature, the tilting and distortion of $Pb_{1-x}Bi_xI_6$ octahedral create the local potential wells for the cations, suppressing the dynamical disordering of $(CH_3NH_3)^+$ cations. As a result, the $CH_3NH_3Pb_{1-x}Bi_xI_3$ structures with symmetry lower than tetragonal class show the ordered orientation of $(CH_3NH_3)^+$ structural units. Experimentally, it was found that $CH_3NH_3Pb_{1-x}Bi_xI_3$ compounds crystallize into monoclinic phase at low temperature [**25**]. Hao *et al.* [**27**] reported a tetragonal $CH_3NH_3Pb_{1-x}Bi_xI_3$ phase at room temperature. However, the unit cell of monoclinic phase deviates from the orthorhombic crystal class very slightly [**26, 28**]. Therefore, one can use an orthorhombic cell to approximate the realistic structure. **Fig. 1** shows the crystal structure of $CH_3NH_3Pb_{1-x}Bi_xI_3$, which is built from $CH_3NH_3Pb_{1-x}Bi_xI_3$ in our previous work [**29**].

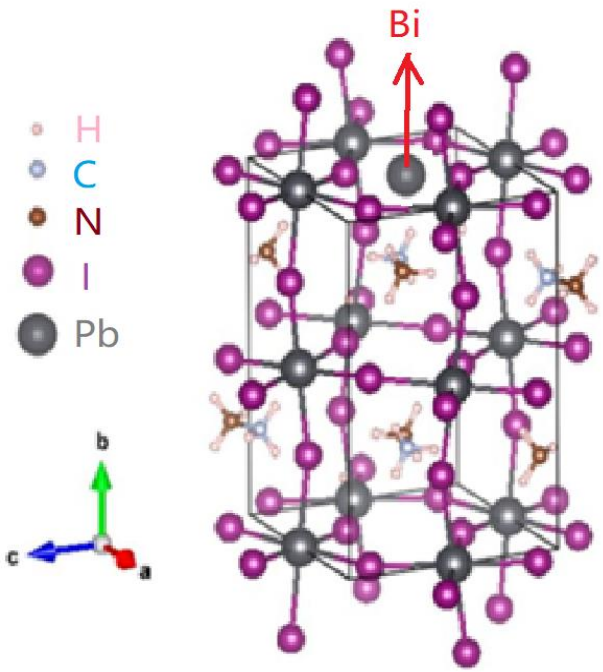

Fig. 1. Crystal structure of $CH_3NH_3Pb_{1-x}Bi_xI_3$

Table 1. Calculated supercell energies and volume and the lattice parameters of undoped and Bi-doped $CH_3NH_3PbI_3$.

Doping concentration	Energy (eV)	Volume (Å^3)	a(Å)	b(Å)	C(Å)
undoped	-15086.82	7858.61	17.60	17.60	25.37
11.1% doping	-16082.23	8007.09	17.61	17.61	25.82
20% doping	-16791.63	8134.08	17.63	17.63	26.17
33.3% doping	-17980.12	8559.90	17.63	17.63	27.54

Results and discussions

We built a 2×2×2 unit cell, and used 4, 2 and 1 Bi atom as the interstitial atoms to insert the unit cell, respectively, the corresponding doping concentration were 33.3%, 20% and 11.1%, respectively. These atom belong the interstitial doped atoms, it is located at the grain boundary. First of all, we optimized the crystal structure, the parameter showed in the **Table 1**, the lattice parameters of Bi-doped CH_3NH_3 $Pb_{1-x}Bi_xI_3$ (x=11.1%, 20%, 33.3%) were a=17.61Å, b=17.61Å, c=25.82Å; a=17.63 Å, b=17.63 Å, c=26.17 Å; a=17.63 Å, b=17.63 Å, c=27.54 Å; their corresponding volume were 8007.09 Å, 8134.08 Å, 8559.90 Å for the doping concentration of 11.1%, 20% and 33.3%, respectively. As we can see, the cell lattice parameter and volume doesn't shift too much, and there is no distortion in the lattice. Then, we calculated the energy band structure and partial density of state (PDOS), as was showed in **Fig. 2 (a-f)**, the doping concentration were 33.3%, 20% and 11.1%, corresponding to the calculated band gap were 0.56 eV, 0.75 eV and 1.46 eV, respectively. It was clear that the bang gap reduced with the doping concentration increased, the reduction lead to the red shift of the $MAPbI_3$'s absorption edge, increased the range of absorption spectrum. In addition, doping induced impurity energy bands closed the Fermi Level, leading to increase of electron density of state near the Fermi Level, which could improve the electrical conductivity. And then, we adopt the exchange correlation energy by GGA-PBE, it is well know that GGA error come from the electrical autocorrelation and internal discontinuity, we have considered the spin-orbit coupling effect between the Pb and I atom in the Bi-doped $CH_3NH_3PbI_3$ system, so the band gap of Bi-doped $CH_3NH_3PbI_3$ was narrower than the experiment result [**30**]. From the PDOS, we found that conduction band near Fermi level mainly constitutes by the electrons on the d orbit of Pb and Bi atom, and the valence band near Fermi level mainly constitutes by the electrons on the p orbit of O atom. After doping, the conduction band become narrower and valance band become much wider as doping concentration addition, consequently, doping induced impurity energy bands main exist in valence band, leading to higher carrier density of state, and more positive Fermi Level.

Copyright © 2019 VBRI Press

What's more, as the Seebeck coefficient (S) driven by the entropy difference depends on temperature, carrier density N(ε) and energetic distribution of electronic states dN(ε)/dε near the Fermi level, as expressed by the following equation:

$$S \sim T\frac{d\ln N(\varepsilon)}{d\varepsilon}\bigg|_{E_F} = T\frac{1}{N(\varepsilon)}\frac{dN(\varepsilon)}{d\varepsilon}\bigg|_{E_F} \quad (1)$$

As we can see from **Fig. 2 (b, d, f)**, the Bi doped perovskite could enlarge the carrier density N(ε) and energetic distribution of electronic states dN(ε)/dε near the Fermi level, so the doped perovskite thin films will exhibit much higher Seebeck coefficient compared with undoped one.

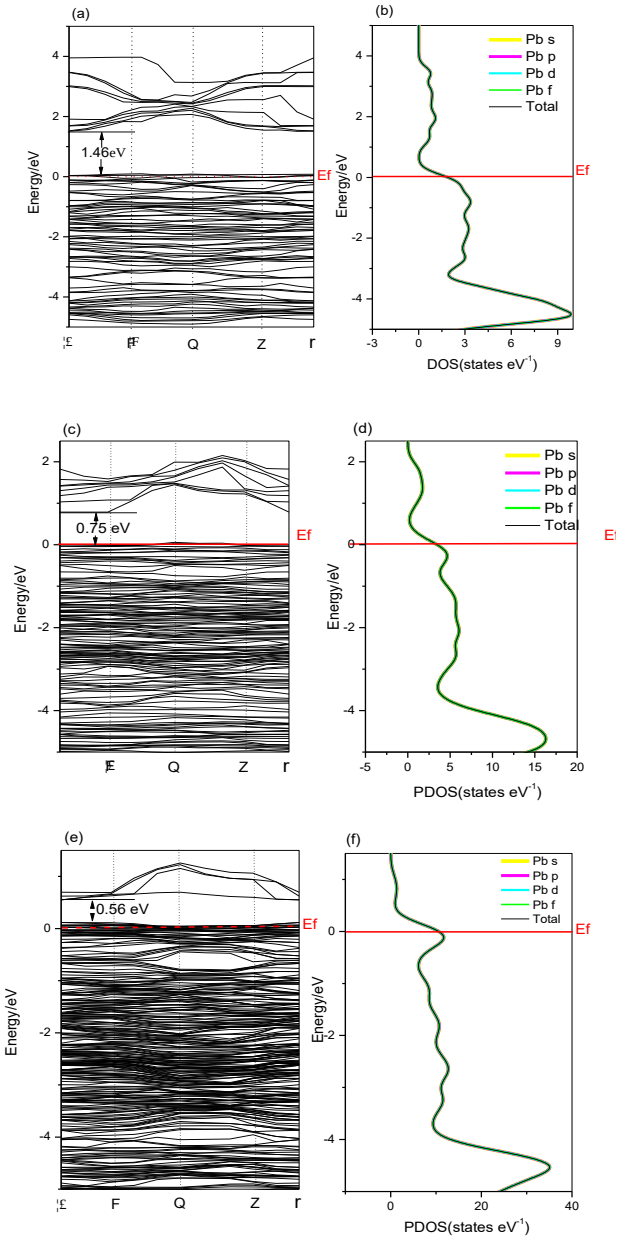

Fig. 2. Different concentration Bi-doped $CH_3NH_3PbI_3$ energy band and density of states, four (a, b), two (c, d), one (e, f) Bi inclusions in a 2×2×2 unit cell, corresponding to 11.1%, 20%, 33.3% doping level.

Moreover, the energy band curve bend degree of conduction band bottom in high concentration Bi dopant (33.3%) is smaller than the low concentration one (11.1%). The carrier effective mass can be derived from the bend of energy band curves, because the inclination of band side was connect with the charge carrier effect mass. We can calculated the charge carrier's effective mass by the energy band's shape, from the equation:

$$m^* = \hbar^2\left[\frac{\partial^2 \varepsilon(k)}{\partial k^2}\right]^{-1} \quad (2)$$

here, Ɛ(k) is the band's average eigenvalue, k is the wave vector, m* is the charge carrier effect mass, m_e* and m_h* are the electron and hole effect mass, respectively, the result showed in **Table 2**. As for the different Bi-doped $CH_3NH_3PbI_3$, the m_e* and m_h* are 1.76 m_0, 3.25 m_0, 5.68 m_0 and the m_h* are 4.12 m_0, 2.79 m_0, 1.53 m_0 for 33.3%, 20%, 11.1% doping concentration, respectively. It is clearly that the effective mass of 11.1% Bi-doped $CH_3NH_3PbI_3$'s charge carrier is the biggest among the doping. From the equation:

$$\mu = \frac{(8\pi)^{1/2}h^4eC_{ii}}{3(m^*)^{5/2}(k_BT)^{3/2}E_1^2} \quad (3)$$

where ħ is Planck constant, e is electron mass, C_{ii} is elastic matrix constant, m* is charge carrier effective mass, k_B is boltzmann constant, T is temperature, E_1 is shape change [**31, 32**]. This equation showed that electron mobility at the high concentration doping (33.3%) was higher than low concentration doping (11.1%), so the Bi-doped $CH_3NH_3PbI_3$'s electrical conductivity can be enhanced with the increased doping concentration, which is in consistence with the experimental result. In addition, the enhanced mobility is also beneficial for higher Seebeck coefficient, because of its mobility was increased. Therefore, we predict that Bi doping can enhance electric conductivity as well as Seebeck coefficient, and could make positive effect on stability.

Table. 2. Calculated band gap and effective masses of Bi-doped $CH_3NH_3PbI_3$.

Doping concentration	Band gap (eV)	Effective mass	
		m^*_e	m^*_h
11.1% doping	1.46	5.68 m_0	4.12 m_0
20% doping	0.75	3.25 m_0	2.79 m_0
33.3% doping	0.56	1.76 m_0	1.53 m_0

Conclusions

The electronic and optical properties of $CH_3NH_3Pb_{1-x}Bi_xI$ (X =11.1%, 20%, 33.3%) perovskites are studied by the first principle calculations using the VASP hybrid functional. The calculated direct band gap of methylammonium bismuth halides ranges from 1.46 to 0.56 eV at the Γ point. The evaluated effective masses of electrons and holes at the same k-point of them are comparable to those of $CH_3NH_3Pb_{1-x}Bi_xI$ materials,

Copyright © 2019 VBRI Press

when the Bi-doped $CH_3NH_3PbI_3$, the structure of Bi as an interstitial atom doped $CH_3NH_3PbI_3$ were much more stable than undoped one by the crystal systemic energy, and the Bi doping made the Fermi Level shift close to the bottom of conduction band, and increased the density of charge carrier near the Fermi level, resulted in the higher electrical conductivity. Moreover, Bi doping produced a smaller electron effective mass with doping concentration addition, increasing the $CH_3NH_3PbI_3$'s mobility. As a result, the Bi-doped $CH_3NH_3PbI_3$ could simultaneously enhance the electrical conductivity and Seebeck coefficient. Our results showed that Bi doped $CH_3NH_3PbI_3$ is a promising approach to develop thermoelectric and photovoltaic properties in organic-inorganic hybrid perovskite materials.

Acknowledgements

We acknowledge financial support from the Hubei province natural science foundation (Grant No: 2016CFB696) and Technology research programme for Hubei province science and technology department (Grant No.03201810302) and Breeding programs Funds for Huanggang Normal University (Grant No: 04201813603).

References

1. Conings, B.; Baeten, L.; De Dobbelaere, C.; D'Haen, J.; Manca, J.; Boyen, H., *Adv. Mater.* **2014**, *26*, 2041. **DOI:** 10.1002/adma.201304803
2. Kojima, A.; Teshima, K.; Shirai, Y.; Miyasaka, T., *J. Am. Chem. Soc.* **2009**, *131*, 6050. **DOI:** 10.1021/ja809598r
3. Park, N., *J. Phys. Chem. Lett.* **2013**, *4*, 2423. **DOI:** 10.1021/jz400892a
4. Snaith, H. J., *J. Phys. Chem. Lett.* **2013**, *4*, 3623. **DOI:** 10.1021/jz4020162
5. Docampo, P.; Ball, J. M.; Darwich, M.; Eperon, G. E.; Snaith, H. J., *Nat. Commun.* **2013**, *4*, 2761. **DOI:** 10.1038/ncomms3761
6. Kim, H. S.; Lee, C. R.; Im, J. H.; Lee, K. B.; Moehl, T.; Marchioro, A.; Moon, S. J.; Humphry-Baker, R.; Yum, J. H.; Moser, J. E.; Gratzel, M.; Park, N. G., *Sci. Rep.* **2012**, *2*, 591. **DOI:** 10.1038/srep00591
7. Ku, Z.; Rong, Y.; Xu, M.; Liu, T.; Han, H., *Sci. Rep.* **2013**, *3*, 3132. **DOI:** 0.1038/srep03132
8. Lee, M. M.; Teuscher, J.; Miyasaka, T.; Murakami, T. N.; Snaith, H. J., *Science*, **2012**, *338*, 6107. **DOI:** 10.1126/science.1228604
9. Liu, M.; Johnston, M. B.; Snaith, H. J., *Nature* **2013**, *501*, 395. **DOI:** 10.1038/nature12509
10. Stranks, S. D.; Eperon, G. E.; Grancini, G.; Menelaou, C.; Alcocer, J. P.; Leijtens, T.; Herz, L. M.; Petrozza, A.; Snaith, H. J., *Science*, **2013**, *342*, 341. **DOI:** 10.1126/science.1243982
11. Burschka, J.; Pellet, N.; Moon, S.; Humphry-Baker, R.; Gao, P.; Nazeeruddin, M. K.; Gratzel, M., *Nature*, **2013**, *499*, 316. **DOI:** 10.1038/nature12340
12. Xing, G.; Mathews, N.; Sun, S.; Lim, S. S.; Lam, Y. M.; Gratzel, M.; Mhaisalkar, S.; Sum, T. C., *Science*, **2013**, *342*, 344. **DOI:** 10.1126/science.1243167
13. Mosconi, E.; Amat, A.; Nazeeruddin, M. K.; Gratzel, M.; De Angelis, F., *J. Phys. Chem. C*, **2013**, *117*, 13902. **DOI:** 10.1021/jp4048659
14. Even, J.; Pedesseau, L.; Jancu, J.; Katan, C., *J. Phys. Chem. Lett.* **2013**, *4*, 2999. **DOI:** 10.1021/jz401532q
15. Mattoni, A.; Filippetti, A., *Phys. Rev. B*, **2014**, *89*, 125203. **DOI:** 10.1103/PhysRevB.89.125203
16. Baikie, T.; Fang, Y. N.; Kadro, J. M.; Schreyer, M.; Wei, F. X.; Mhaisalkar, S. G.; Graetzel, M.; White, T. J., *J. Mater. Chem. A*, **2013**, *1*, 5628. **DOI:** 10.1039/C3TA10518K
17. Gidlow, D. A., Lead toxicity. Occup. Med. **2004**, *54*, 76. **DOI:** 10.1093/occmed/kqh019
18. Heyd, J.; Scuseria, G. E.; Ernzerhof, M., *J. Chem. Phys.* **2003**, *118*, 8207. **DOI:** 10.1063/1.1564060
19. Dion, M.; Rydberg, H.; Schröder, E.; Langreth D. C.; Lundqvist, B. I., *Phys. Rev. Lett.*, **2004**, *92*, 246401. **DOI:** 10.1103/PhysRevLett.92.246401
20. Blöchl, P. E.; Jepsen O.; Andersen, O. K., *Physi. Rev. B* **1994**, *49*, 16223. **DOI:** 10.1103/PhysRevB.49.16223
21. Onoda-Yamamuro, N.; Matsuo, T.; Suga, H., *J. Phys. Chem. Solids*, **1990**, *51*, 1383. **DOI:** 10.1016/0022-3697(90)90021-7
22. Mashiyama, H.; Kurihara, Y.; Azetsu, T., *J. Korean Phys. Soc*. **1998**, *32S*, S156.
23. Kawamura, Y.; Mashiyama, H.; Hasebe, K., *J. Phys. Soc. Jpn*. **2002**, *71*, 1694. **DOI:** 10.1143/jpsj.71.1694
24. Borriello, I.; Cantele, G.; Ninno, D., *Phys. Rev. B*, **2008**, *77*, 23521423. **DOI:** 10.1103/PhysRevB.77.235214
25. Chiarella, F.; Zappettini, A.; Licci, F.; Borriello, I.; Cantele, G.; Ninno, D.; Cassinese, A.; Vaglio, R., *Phys. Rev. B*, **2008**, *77*, 0451294. **DOI:** 10.1103/PhysRevB.77.045129
26. Stoumpos, C. C.; Malliakas, C. D.; Kanatzidis, M. G., *Inorg. Chem.*, **2013**, *52*, 9019. **DOI:** 10.1021/ic401215x
27. Hao, F.; Stoumpos, C. C.; Cao, D. H.; Chang, R. P. H.; Kanatzidis, M. G., *Nat. Photonics*, **2014**, *8*, 489. **DOI:** 10.1038/nphoton.2014.82
28. Takahashi, Y.; Obara, R.; Lin, Z. Z.; Takahashi, Y.; Naito, T.; Inabe, T.; Ishibashi, S.; Terakura, K., *Dalton Trans.*, **2011**, *40*, 5563. **DOI:** 10.1039/C0DT01601B
29. Feng, J.; Xiao, B., *J. Phys. Chem. Lett*., **2014**, *5*, 1278. **DOI:** 10.1021/jz500480m
30. Abdelhady, A. L.; Saidaminov, M. I.; Murali, B.; Adinolfi, V; Voznyy, O.; Katsiev, K.; Alarousu, E.; Comin, R.; Dursun, I.; Sinatra, L.; Sargent, E. H.; Mohammed, O. F.; Bakr, O. M., *J. Phys Chem Lett.,* **2016**, *7,* 295. **DOI:** 10.1021/acs.jpclett.5b02681
31. Stoumpos, C. C.; Malliakas, C. D.; Kanatzidis, M. G., Semiconducting tin and lead iodide perovskites with organic cations: phase transitions, high mobilities, and near-infrared photoluminescent properties. *Inorganic Chemistry,* **2013,** *52,* 9019. **DOI:** 10.1021/ic401215x
32. Franceschetti, A.; Wei, S. H.; Zunger, A., *Phys. Revi. B,* **1994**, *50,* 17797. **DOI:** 10.1103/PhysRevB.50.17797

Copyright © 2019 VBRI Press